Pol. J. Environ. Stud. Vol. XX, No. X (XXXX), 1-14
DOI: *10.15244/pjoes/220125* ONLINE PUBLICATION DATE: 2026-07-28

Original Research

Preparation of Novel TiO_2-RNTs/SnO_2-Sb/PbO_2-La Electrode and Degradation of Oily Wastewater by Pulse Electrochemical Advanced Oxidation Process

Yachao Han#, Yunlei Cen#, YuanYuan Zhou, Ke Zheng, Shaoqi Zhou*

College of Resources and Environmental Engineering, Guizhou University, Guiyang 550025, China

Received: 21 November 2025
Accepted: 27 March 2026

Abstract

The novel TiO_2-RNTs/SnO_2-Sb/PbO_2-La electrode was prepared by electrodeposition, and its performance was better than that of the Ti/SnO_2-Sb/PbO_2 electrode: it had a denser structure, higher oxygen evolution potential (1.65 V), larger electrochemical active surface area (EASA = 138.47), lower charge transfer resistance (5.4 Ω), and longer electrode strengthening life (960 min). Under the optimal conditions, the degradation rate increased by 1.4 times, the oil removal rate was 95.65%, and the removal rate remained stable after 10 cycles. The failed electrode was re-prepared, and the oil removal rate could still reach more than 95%. Compared with direct current, pulse current electrolysis of wash oil wastewater can save 54.61% of electric energy and 76.80% of energy consumption per unit mass of COD removal. Therefore, the pulse electrochemical oxidation method using the TiO_2-RNTs/SnO_2-Sb/PbO_2-La electrode is expected to improve the electrochemical treatment of oily wastewater while reducing unnecessary energy loss.

Keywords: TiO_2 nanotubes, La doping modification, wash oil, pulse electrochemical oxidation, saving energy

Introduction

Wash oil is a kind of yellowish-brown or brown oily liquid, which is rich in naphthalene, fluorene, acenaphthene, and other unique alkanes and polycyclic aromatic hydrocarbons. It is the absorption oil of benzene or naphthalene compounds washed out from gas, and it is also the main fraction of coal tar and oil. Once leaked, it will cause serious pollution to groundwater, air, farmland, and organisms. These compounds are highly toxic, and long-term and acute exposure may cause harmful health disorders in humans [1]. Therefore, it is urgent to develop an effective and economical method for the treatment of oily wastewater.

Advanced oxidation processes (AOPs), such as photocatalytic oxidation [2, 3], Fenton oxidation [4-6], and electrocatalytic oxidation [7-9], generate hydroxyl radicals with a high redox potential (2.8 V), enabling the non-selective degradation of pollutants and making them suitable for the treatment of oily wastewater composed of many kinds of pollutants. Among them, electrocatalytic oxidation technology has become one of the most promising advanced oxidation technologies for wastewater treatment due to its advantages of non-

# equal contribution
*e-mail: zhousq@gzu.edu.cn

selectivity, high oxidation efficiency, and environmental friendliness [10, 11]. It has been widely used in oily wastewater [7-9, 12-15]. The PbO_2 electrode based on titanium is considered to be an attractive anode because of its easy electrodeposition, low energy consumption, long service life, and good pollutant removal performance [16].

The Ti/PbO_2 electrode is generally optimized from three aspects: the titanium matrix, the intermediate layer, and the active layer. It can be clearly seen from previous reports that the highly ordered, vertically oriented, large surface area, and good hydrophilicity of TiO_2 nanotubes (TiO_2-NTs) formed by oxidation on the Ti substrate enhance the effectiveness of the PbO_2 top layer in electrode stability [17, 18]. The Sb-SnO_2 interlayer can reduce the internal stress between the PbO_2 and the substrate, thereby enhancing the conductivity of the PbO_2 electrode [19]. Meanwhile, introducing foreign atoms or active particles into the active layer of PbO_2 or PbO_2-based electrodes enhances electrocatalytic performance. Specifically, doping rare earth elements (e.g., La [20], Ce [21]), metal oxides (e.g., Fe [22], Co [23], Ni [24], Cu [25]), or non-metals (e.g., Si_3N_4 [26], GN [27]) has been shown to improve the stability and electrocatalytic activity of PbO_2 electrodes. For example, a lanthanum (La) doped PbO_2 electrode has longer service life, higher oxygen evolution overpotential, and better electrocatalytic performance.

In addition to the anode material, current is another key factor in the electrochemical oxidation process, because it directly determines the oxidation efficiency and energy consumption. Traditional electrochemical systems usually conduct electrolysis of pollutants in constant potential or constant current mode, which may lead to low efficiency or selectivity [27]. In such an electrolysis mode, sustainable electricity is consumed, leading to unsatisfactory energy efficiency. In this case, pulse electrolysis has become the focus of attention due to its tunability of the electrode-electrolyte interface properties [28]. In the pulse current mode, a pulse period includes turn-on time (t_{on}) and turn-off time (t_{off}). When the current is periodically turned off, ions or electrolytes can easily move to the electrode surface to promote mass transfer and save energy [27-29]. In addition, pulse electrolysis has been shown to inhibit anode passivation [30]. Therefore, pulsed electrochemical oxidation is considered to be a potential alternative to improve energy efficiency [27-29].

In summary, we further enhanced the surface of the pretreated Ti substrate by using two anodic oxidations and one cathodic reduction, improved the interfacial electron transfer between the substrate and the metal oxide coating, and produced reduced TiO_2-RNTs on the surface [17, 19]. The SnO_2-Sb intermediate layer was prepared by the hydrothermal method. Finally, the α-PbO_2 intermediate layer and the rare metal La-doped modified β-PbO_2 active layer were prepared by electrodeposition. The physical and chemical (SEM, XPS, XRD), and electrochemical properties (LSV, CV, EIS), were characterized. The morphology, structure, and electrochemical properties of the novel TiO_2-RNTs/SnO_2-Sb/PbO_2-La electrode were analyzed, and then the oxidation efficiency and energy efficiency of wash oil degradation were used to evaluate the application potential of pulse electrolysis.

Materials and Methods

Laboratory Chemicals and Oily Wastewater

Titanium plate (purity > 99.9%) was purchased from Changjiang Titanium Industry Co., Ltd., China. All other chemicals used in this study were of analytical grade except for those labeled otherwise. Lead nitrate (GR) was purchased from Chongqing Chuandong Chemical Co., Ltd., China. Lead oxide, lanthanum nitrate (III) hexahydrate, antimony trichloride, ethylene glycol, anhydrous ethanol, isopropanol, anhydrous oxalic acid, and anhydrous sodium sulfate were purchased from Aladdin. Tin tetrachloride (IV) pentahydrate, copper nitrate, sodium fluoride, tert-butyl alcohol, and glass wool were purchased from Macklin. All experiments were performed using ultrapure water (18.25 MΩ cm from the Milli-Q system).

The wash oil wastewater used in this experiment was provided by Jinan Yingxin Chemical Co., Ltd. The preparation method of emulsified oil and the details of its composition of 48 organic compounds are shown in our previous study [31].

Electrode Preparation

The electrode consists of three parts: Ti substrate, intermediate layer (TiO_2-RNTs, SnO_2-Sb, α-PbO_2), and β-PbO_2-La active layer. Fig. 1a) is the structure of the TiO_2-RNTs/SnO_2-Sb/PbO_2-La electrode. TiO_2 nanotubes, which are called TiO_2-RNTs, were prepared by using two anodic oxidations and one cathodic reduction [17, 19]. The pretreatment of the Ti substrate and the detailed preparation method of TiO_2-RNTs are shown in text S1.

In order to reduce the stress of TiO_2 nanotubes, a TiO_2-RNTs/SnO_2-Sb electrode was prepared by the hydrothermal method. Firstly, 5.2590 g (15 mmol) $SnCl_4$ $5H_2O$ and 0.3422 g (1.5 mmol) $SbCl_3$ were added to a 150 mL anhydrous ethanol solution, and the mixture was ultrasonically stirred. Then, the mixture and the Ti/TiO_2-RNTs electrode were transferred to a 300 mL PTFE-lined stainless steel autoclave for sealing. After 15 min of ultrasonic treatment to remove residual bubbles from the nanotubes, they were heated at 180ºC for 12 h. After that, the electrode was washed repeatedly with water and ethanol, then calcined at 500ºC for 2 h in air to obtain the TiO_2-RNTs/SnO_2-Sb electrode.

The TiO_2-RNTs/SnO_2-Sb/PbO_2-La electrode was prepared by co-deposition of PbO_2 coating and

La on the TiO_2-RNTs/SnO_2-Sb electrode using two electrodeposition methods. During the electrodeposition process, the prepared electrode was placed as an anode, and the polished, smooth titanium plate was used as a cathode. The α-PbO_2 interlayer was deposited at room temperature with 20 mA cm^{-2} in a 150 mL mixed electrolyte solution containing 0.1 mol L^{-1} PbO and 3.5 mol L^{-1} NaOH for 60 min. Then the β-PbO_2-La active layer was deposited at 60ºC for 60 min in 150 mL electrolyte solution composed of 0.5 mol L^{-1} $Pb(NO_3)_2$, 0.5 g L^{-1} NaF, 0.005 mol L^{-1} $La(NO_3)_3$, 0.005 mol L^{-1} $Cu(NO_3)_2$, and 0.1 mol L^{-1} HNO_3. Among them, F-doping can prevent the diffusion of free oxygen atoms into the PbO_2 structure and provide a stable activity of the anode [32]. Cu^{2+} incorporation can accurately control the amount of Pb generated by Pb^{2+} cathode reduction and prevent the deposition of Pb through the preferential deposition of Cu [33]. In particular, Cu^{2+} inhibits the vertical growth of dendritic Pb at the cathode and reduces the risk of interference on the anode PbO_2 surface because it forms a copper film on the cathode surface.

In order to compare, the TiO_2-RNTs/SnO_2-Sb/PbO_2 electrode without La and Cu in the electrolyte was prepared according to the above process, and the Ti/SnO_2-Sb/PbO_2 electrode was prepared on the Ti plate.

Electrode Characterization

Scanning electron microscopy (SEM, ZEISS Sigma 360, Germany) equipped with energy dispersive X-ray spectroscopy (EDS) was used to study the surface morphology and microstructure of the prepared electrode. X-ray diffraction (XRD, Rigaku SmartLab SE, Japan) was used to characterize the phase structure of the electrode. X-ray photoelectron spectroscopy (XPS, Thermo Scientific K-Alpha, USA) was performed to determine the surface chemical state and elemental composition of the prepared electrode.

All electrochemical tests were performed on an electrochemical workstation (CHI 650E, CHI Shanghai, Inc., China). The prepared electrode with an effective area of 2×2 cm^2 was used as the working electrode, and the platinum electrode and the saturated calomel electrode were used as the counter electrode and the reference electrode, respectively. Linear sweep voltammetry (LSV), cyclic voltammetry (CV), and electrochemical impedance spectroscopy (EIS) tests were performed in 200 mL 0.25 mol L^{-1} sodium sulfate solution. The LSV test was performed at a scan rate of 20 mV s^{-1} in the voltage range of 0-2.4 V. CV tests were performed at different scan rates (10-100 mV s^{-1}) between 0.3 V and 1.6 V. The EIS test was carried out in the test frequency range of 0.1 Hz to 10^5 Hz, the maximum amplitude was 5 mV, and the test potential was 1.5 V (vs. SCE). Accelerated electrode life tests of different electrodes were performed using a two-electrode system. Constant current electrolysis was carried out in 1.0 mol L^{-1} sulfuric acid solution at a current density of 1.0 A cm^{-2} during the tests. The electrode potential was recorded every 30 min, and the electrode was considered inactivated when its potential increased by 5 V compared with the initial value [34].

Electrochemical Degradation Experiment

The prepared electrode and polished titanium plate were used as the anode and cathode, respectively. In a single-chamber electrolytic cell containing 250 mL treatment solution, the electrochemical degradation test was carried out under the conditions of oil wastewater concentration of 100 mg L^{-1}, temperature of 30ºC and stirring at 300 rpm (Fig.1b)). Different initial pH values, current density, electrode spacing, pulse frequency, and pulse duty cycle were discussed. 2 mL samples were taken at intervals and immediately used for subsequent analysis.

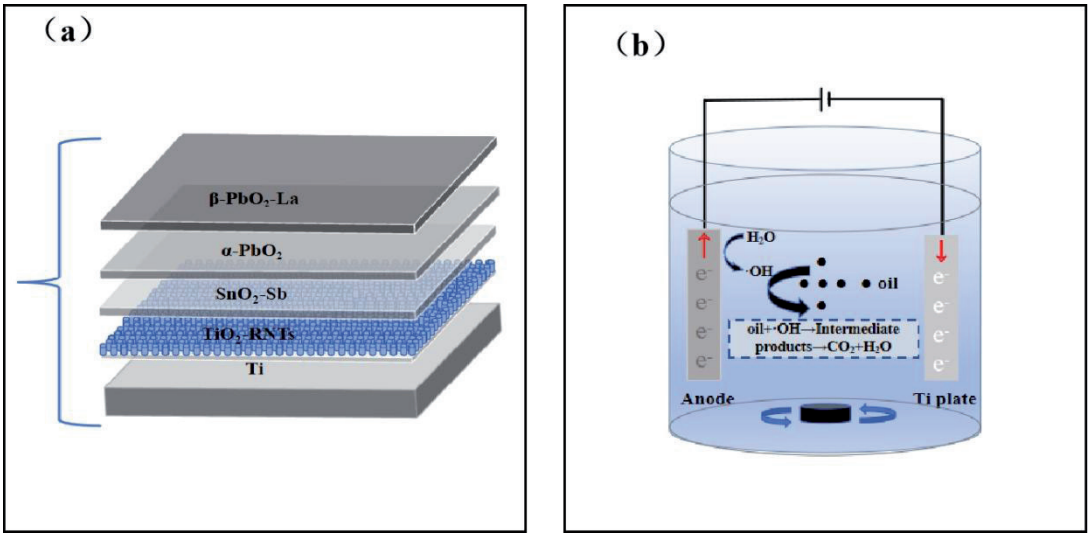

Fig. 1. The structure of the TiO_2-RNTs/SnO_2-Sb/PbO_2-La electrode.

A UV-Vis spectrometer (Jasco, V670, Japan) was used to measure the content of oil in wastewater and the content of COD in oily wastewater at 225 nm and 440 nm, respectively. The standards are "Determination of petroleum in water by ultraviolet spectrophotometry" (HJ 970-2018) and "Determination of chemical oxygen demand in water by rapid digestion spectrophotometry" (HJ/T 399-2007). Total organic carbon (TOC) was measured in a TOC analyzer (Enviro TOC, Germany). The concentration of metal ions in the solution was determined by ICP-OES/MS (Agilent 7800 (MS), USA). Various organic compounds in the solution before and after electrolysis were determined using a 7890A-5975C gas chromatograph-mass spectrometer ((GC-MS), Agilent Technologies, Inc., USA).

According to the change of wash oil concentration, the degradation efficiency of wash oil is calculated by the following Equation (1):

$$Degradationefficiency(\%) = \frac{C_0 - C_t}{C_0} \times 100 \quad (1)$$

The degradation of wash oil in this study can be well fitted with pseudo-first-order kinetics, which uses the following Equation (2):

$$\ln(\frac{C_t}{C_0}) = -kt \quad (2)$$

Where k is the reaction rate constant (min^{-1}), and t is the discharge time (min).

The reduced current efficiency (EE/O) per logarithmic order is the energy consumption (kWh m^{-3}) required to degrade the target pollutants in 1 m^3 of polluted water matrix, which is expressed by the following Equation (3) [22]:

$$EE/O = \frac{\varphi UIt}{V \log(\frac{C_0}{C_t})} \quad (3)$$

In the formula, φ, U, I, t, and V are the duty cycle of the power pulse, the applied voltage (kV), the current (A), the discharge time (h), and the amount of wastewater (m^3), respectively. The EE/O formula is only applicable to the degradation process of the pseudo-first-order kinetic model.

The energy consumption for COD removal per unit mass (E_{sp}, kWh kg^{-1}_{COD}) is calculated as follows (4):

$$E_{sp} = \frac{\varphi^2 UIt}{mV} \quad (4)$$

Where m is the mass of COD removed (kg).

Results and Discussion

Characterization of the Prepared Electrode

Fig. 2a) is the SEM image of TiO_2-RNTs. It can be seen that the compact TiO_2 nanoarray tubes are stacked on the surface of the titanium sheet. After the formation of TiO_2-RNTs, the specific surface area increased significantly, which could improve the adhesion and loading of the Sb-SnO_2 interlayer. Fig. 2b) shows that the tiny and irregular particles of SnO_2-Sb adhere to each other, and the compact TiO_2 nanoarray tube has been completely covered by the SnO_2-Sb coating. Fig. 2c) and its illustrations show that the outermost layer has a typical pyramid structure, and the surface β-PbO_2 particles are dense and uniform. There are many visible cracks on the electrode surface, and the active surface layer is easy to peel off, which will shorten the electrode life. In contrast, when La is doped on the surface, the pyramid structure of β-PbO_2 becomes smooth and uniformly dispersed, which significantly reduces the cracks between PbO_2 crystals and makes the electrode surface denser. This indicates that the doping of La_2O_3 effectively limits the growth of β-PbO_2 particles and is used to enhance the electrocatalytic performance of the anode. The EDX of TiO_2-RNTs/SnO_2-Sb/PbO_2-La electrode and the distribution and content of elements on the electrode surface are shown in Fig. 2e) and its illustration. The At% of O and Pb is about 2:1, which confirms the existence of PbO_2. The presence of the La element was detected, indicating that the doping was successful.

XRD was used to determine the crystal structure of the TiO_2-RNTs/SnO_2-Sb/PbO_2-La electrode (Fig. 2f)). The results show that the electrode is mainly composed of a tetragonal crystal structure. The main diffraction peaks at 25.2°, 31.9°, 31.7°, 48.8°, and 62.2° are attributed to the (110), (101), (200), (211), and (301) crystal planes of β-PbO_2, respectively. These major diffraction peaks are largely consistent with the standard data for reference card number JCPD 7544-900-96. The remaining diffraction peaks may belong to La or other impurities. No diffraction peak of TiO_2 was observed on the electrode, indicating that the electrode surface was completely occupied by β-PbO_2, which was consistent with the SEM image.

XPS was used to analyze the chemical state on the electrode surface (Fig. 3(a-c)). Cu cannot be detected by XPS because the amount of $Cu(NO_3)_2$ added in the electrolyte is very small, and Cu is preferentially deposited on the cathode. Organic carbon pollution was identified as the reason for the presence of the C element on the electrode surface. In order to determine the bonding state of elements, Avantage software was used to separate peaks to fit the high-resolution peaks of O 1s, Pd 4f, and La 3d spectra, in which the binding energy was calibrated relative to the carbon C 1s peak at 284.80 eV.

The peaks at 529.31 eV, 531.38 eV, and 532.58 eV in the O 1s spectrum of Fig. 3a) are attributed to lattice

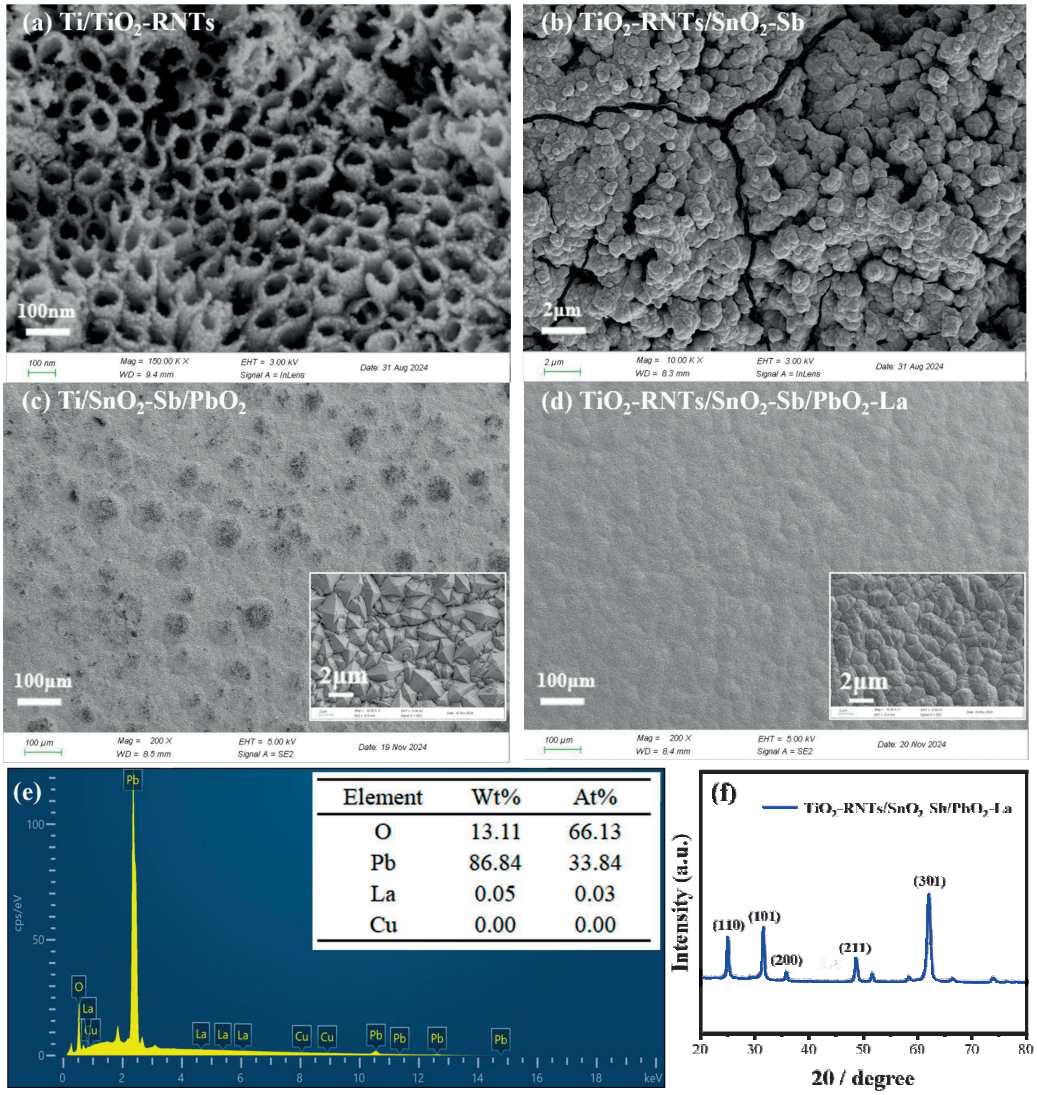

Fig. 2. The SEM images of a) Ti/TiO_2-RNTs, b) TiO_2-RNTs/SnO_2-Sb electrode, c) Ti/SnO_2-Sb/PbO_2 electrode, and d) TiO_2-RNTs/SnO_2-Sb/PbO_2-La electrode; e) the EDS spectrum and the corresponding element content distribution of the Ti/TiO2-RNTs/SnO2-Sb/PbO2-La electrode; f) the XRD pattern of the TiO2-RNTs/SnO_2-Sb/PbO_2-La electrode.

oxygen (O_{lat}) and additional oxygen (O_{ads}), respectively. O_{lat} represents the oxygen species in the PbO_2 lattice, and Oads are usually related to adsorbed oxygen and weakly bound hydroxyl groups [35]. The presence of these substances enhances the catalytic performance of the electrode and helps to oxidize organic pollutants by generating more ·OH on the anode surface [36]. The Pb 4f spectra in Fig. 3b) show peaks at 142.18 eV and 137.45 eV, attributed to Pb $4f_{5/2}$ and Pb $4f_{7/2}$, which are derived from Pb^{4+} and Pb^{2+} [37-39]. These peaks reveal the existence of PbO_2 and PbO in the TiO_2-RNTs/SnO_2-Sb/PbO_2-La electrode and the Ti/SnO_2-Sb/PbO_2 electrode. The atomic ratio of Pb^{4+}/Pb^{2+} was calculated according to the peak area in XPS. As shown in Table S4, the ratio of Pb^{4+}/Pb^{2+} in the TiO_2-RNTs/SnO_2-Sb/PbO_2-La electrode (8.27) is greater than that in the Ti/SnO_2-Sb/PbO_2 electrode (3.27), indicating that the addition of La and Cu in the electrolyte solution promotes the anodic oxidation of Pb^{2+} to Pb^{4+} and the subsequent formation of PbO_2, and reduces the surface precipitation of PbO. Multiple peaks appear in Fig. 3c), and the four binding energies corresponding to La 3d are 855.78 eV, 853.38 eV, 840.78 eV, and 836.78 eV, respectively, indicating that La exists in the form of La_2O_3 or $La(OH)_3$.

Electrochemical Properties of the Prepared Electrode

OEP is an important key to evaluating the side reaction of oxygen evolution. Higher OEP can better inhibit the oxygen evolution reaction and improve the current efficiency [40]. As shown in Fig. 4a), the OEP (V vs. SCE) of Ti/SnO_2-Sb/PbO_2, TiO_2-RNTs/SnO_2-Sb/PbO_2, and TiO_2-RNTs/SnO_2-Sb/PbO_2-La electrodes are 1.52 V, 1.62 V, and 1.65 V, respectively. The work of TiO_2-RNTs/SnO_2-Sb/PbO_2-La was compared with some electrodes reported in recent studies (Table 1). It

Table 1. OEP comparisons for some anodes reported in recent studies.

Anodic materials	OEP (V vs. SCE)	Refs.
TiO_2-RNTs/SnO_2-Sb/PbO_2-La	1.65	This work
Ti/SnO_2–Sb/PVDF-PbO_2-ZrO_2	1.63	[8]
Ti/SnO_2-Sb/PbO_2	1.54	[20]
Ti/SnO_2-Sb/PbO_2-La	1.63	[20]
Ti/SnO_2–Sb/Co-βPbO_2	1.57	[49]
Ti/TiO_2-NTs/PbO_2	1.52	[50]
Ti/TiO_2-NTs/Sb-SnO_2/PbO_2	1.60	[50]

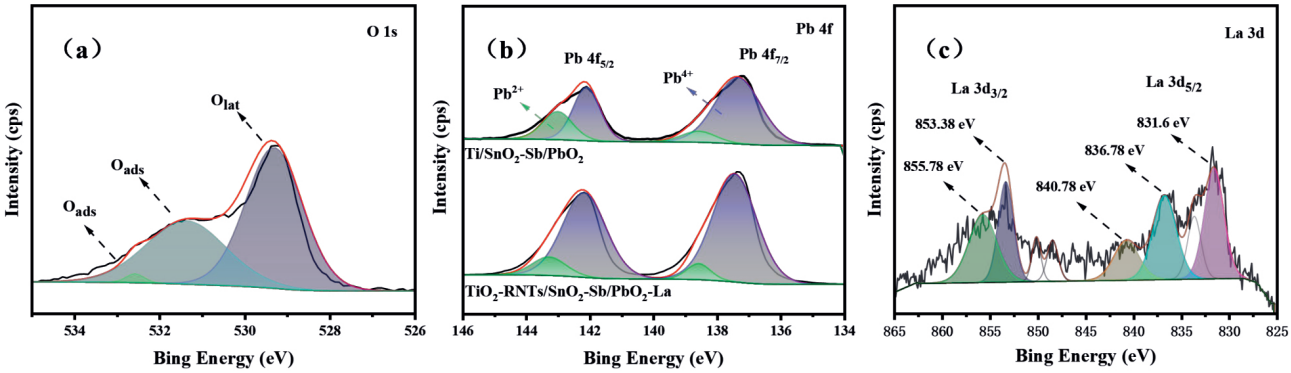

Fig. 3. The detailed XPS spectra of a) O 1s, b) Pd 4f, and c) La 3d.

shows that the introduction of an intermediate layer, TiO_2-RNTs, and La doping modification increases the OEP of the electrode, resulting in more ·OH and inhibiting the oxygen evolution side reaction, which is beneficial to the degradation of organic matter.

The CVs of Ti/SnO_2-Sb/PbO_2 and TiO_2-RNTs/SnO_2-Sb/PbO_2-La electrodes in 0.25 mol L^{-1} Na_2SO_4 at different scan rates (10-100 mV s^{-1}) are shown in Fig. 4b) and 4c) to study the active sites of the prepared electrodes. The peak current density of all electrodes has a good linear ratio and increases with the increase of the scanning rate. The oxidation peak and reduction peak appeared in the curve, representing the oxidation and reduction of Pb^{2+}/Pb^{4+} in the electrode film, respectively, which proved that the reversible reaction occurred. Voltammetric charge (q*, mC cm^{-2}) and electrochemically active surface area (EASA) are important indicators of electrocatalytic performance. In Fig. 4b) and 4c), the integral area of the 10 mV s^{-1} CV curve at 10 mV s^{-1} can calculate the q* value of the electrode, and the q* value of the TiO_2-RNTs/SnO_2-Sb/PbO_2-La electrode is 70.38 mC cm^{-2}. It is 1.21 times that of the Ti/SnO_2-Sb/PbO_2 electrode. The current density of the CV curve at different scan rates (10-100 mV s^{-1}) corresponding to 0.95 V was fitted, and the double-layer capacity (CDL) was calculated using Equation (5), as shown in Fig. 4d). EASA was estimated using Equation (6) [34, 41].

$$I_C = VC_S \quad (5)$$

$$EASA = C_{DL} / C_S \quad (6)$$

Among them, I_C, V, $C_{DL,}$ and C_S represent the non-Faradaic capacitive current, scanning rate, double-layer capacitance, and specific capacitance of a smooth flat surface, respectively. For ease of calculation, the specific capacitance is regarded as a constant value of 50 μF cm^{-2} [41]. Through calculation, the EASA of the TiO_2-RNTs/SnO_2-Sb/PbO_2-La electrode is 199.4, which is 1.44 times that of the Ti/SnO_2-Sb/PbO_2 electrode (EASA = 138.47). The surface activity increased. Therefore, it can be considered that La element has a greater synergistic effect on the surface-active center of PbO_2, which improves the anode activity. This further promotes the oxidation reaction.

The Nyquist diagram and the corresponding equivalent circuit fitted by ZView software are shown in Fig. 4e). Rs, Rct, and CPE are solution resistance, charge transfer resistance, and constant phase element, respectively. The Rct of the TiO_2-RNTs/SnO_2-Sb/PbO_2-La electrode was 5.4 Ω, which was 0.1 Ω lower than that of the Ti/SnO_2-Sb/PbO_2 electrode. This means that the appropriate amount of La doping helps to enhance the conductivity of the electrode, thus improving the apparent electrocatalytic activity of the electrode.

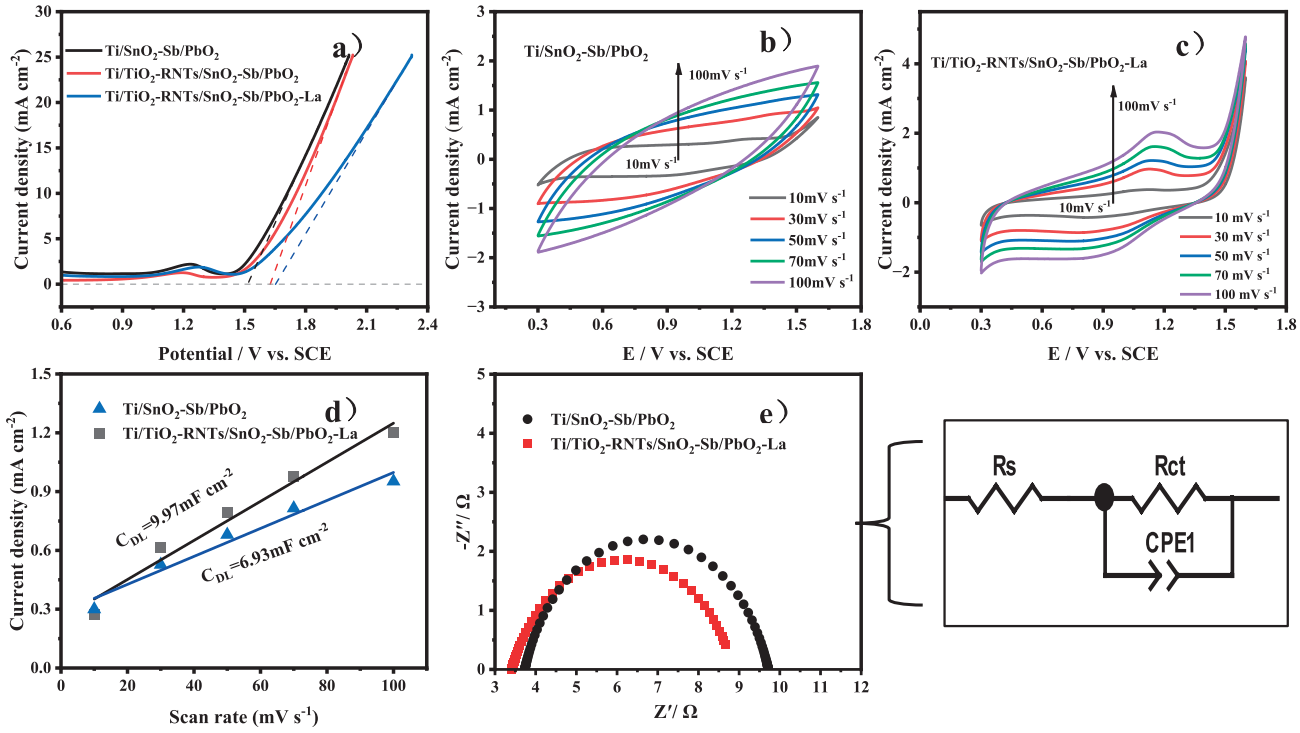

Fig. 4. a) The LSV curve of three PbO_2 electrodes; b) The CV curve of the Ti/SnO_2-Sb/PbO_2 electrode at a scan rate of 10-100 mV s^{-1}; c) The CV curve of the TiO_2-RNTs/SnO_2-Sb/PbO_2-La electrode at a scan rate of 10-100 mV s^{-1}; d) The CDL value of the electrode before and after modification, and the current density of the CV curve at 0.95 V corresponding to different scanning rates; e) The EIS of the electrode before and after modification.

Electrochemical Oxidation of Oily Wastewater

Effects of Operating Parameters on Pulse Electrochemical Oxidation Performance

In a single-chamber electrolytic cell containing 250 mL of the treated solution, the electrochemical degradation of oil-washing wastewater with different initial pH values, current density, electrode spacing, pulse frequency, and pulse duty cycle was investigated. Firstly, the effect of pH on the degradation of oily wastewater in a pulse electrochemical system was studied. The results in Fig. 5a) show that the acidic conditions are beneficial to the electrochemical degradation of wash oil wastewater. When the pH increased from 3 to 9, the degradation rate of wash oil wastewater gradually decreased from 0.0187 min^{-1} to 0.0127 min^{-1}. This is because acidic conditions are conducive to the formation of ·OH and inhibit the release of oxygen, which improves the utilization of ·OH for the decomposition of wash oil components [42]. It has been reported that more free radicals can be produced under acidic conditions [43]. Under alkaline conditions, ·OH can be removed by OH^-, showing low reactivity to organic matter [20]. Therefore, pH = 3 was selected for further study.

The results in Fig. 5b) showed that when the current density increased from 10 mA cm^{-2} to 20 mA cm^{-2}, the degradation rate of oil-containing wastewater increased significantly with the increase of current density, and the degradation efficiency of oil-containing wastewater increased from 81.03% to 95.65%. When the current density continued to increase, the degradation rate k decreased. This is because too high current density will lead to an increase in the rate of side reactions (O_2 and H_2 precipitation), resulting in a decrease in current efficiency [44]. Therefore, the current density of 20 mA cm^{-2} was selected for further research.

The results of Fig. 5c) show that when the electrode plate spacing is reduced from 30 mm to 10 mm, the removal rate and the k value of the wash oil wastewater are greatly improved, and the cell voltage is found to be reduced. At a lower electrode distance, there is a shorter diffusion distance between the electrodes for more efficient electrolysis. However, a very small electrode distance can easily lead to potential safety hazards, such as uneven distribution of wash oil wastewater and short circuit of the electrodes [45]. Therefore, the electrode spacing of 10 mm was selected for further research.

The results of Fig. 5d) showed that when the pulse frequency increased from 1000 Hz to 7000 Hz, the removal rate of wash oil exceeded 90.0% after 180 min of reaction. The highest wash oil removal (95.65%) and the maximum reaction rate (k = 0.0187 min^{-1}) were achieved at a pulse frequency of 5000 Hz. This may be because a higher pulse frequency can reduce the turn-on time in the pulse period and improve the mass transfer process, thereby promoting the utilization of ·OH and

reducing the binding reaction between ·OH radicals [46]. When the pulse frequency reaches 7000 Hz, it is found that the degradation efficiency decreases, indicating that too high a pulse frequency will lead to pulse regression or be meaningless. Therefore, the pulse frequency of 5000 Hz is selected for further research.

Fig. 5e) shows that as the pulse duty cycle increases from 10% to 50%, the wash oil removal rate increases rapidly. The results can be explained by the fact that when the pulse frequency is set to a constant value, a larger pulse duty cycle means a longer electrochemical reaction time and more ·OH is formed on the electrode surface [47]. However, when the duty cycle exceeds 50%, a slight decrease in the removal rate was observed from 50% to 70% and then to the DC power supply (DC). Aiming at the phenomenon that the removal rate of wash oil with a pulse duty cycle of 50% is greater than that under DC electrolysis, we reduced the current density to 10 mA cm^{-2}. As shown in Fig. 5f), the removal rate under DC electrolysis is significantly greater than that of the 50% pulse duty cycle. Therefore, we speculate that they have a critical point of equal removal

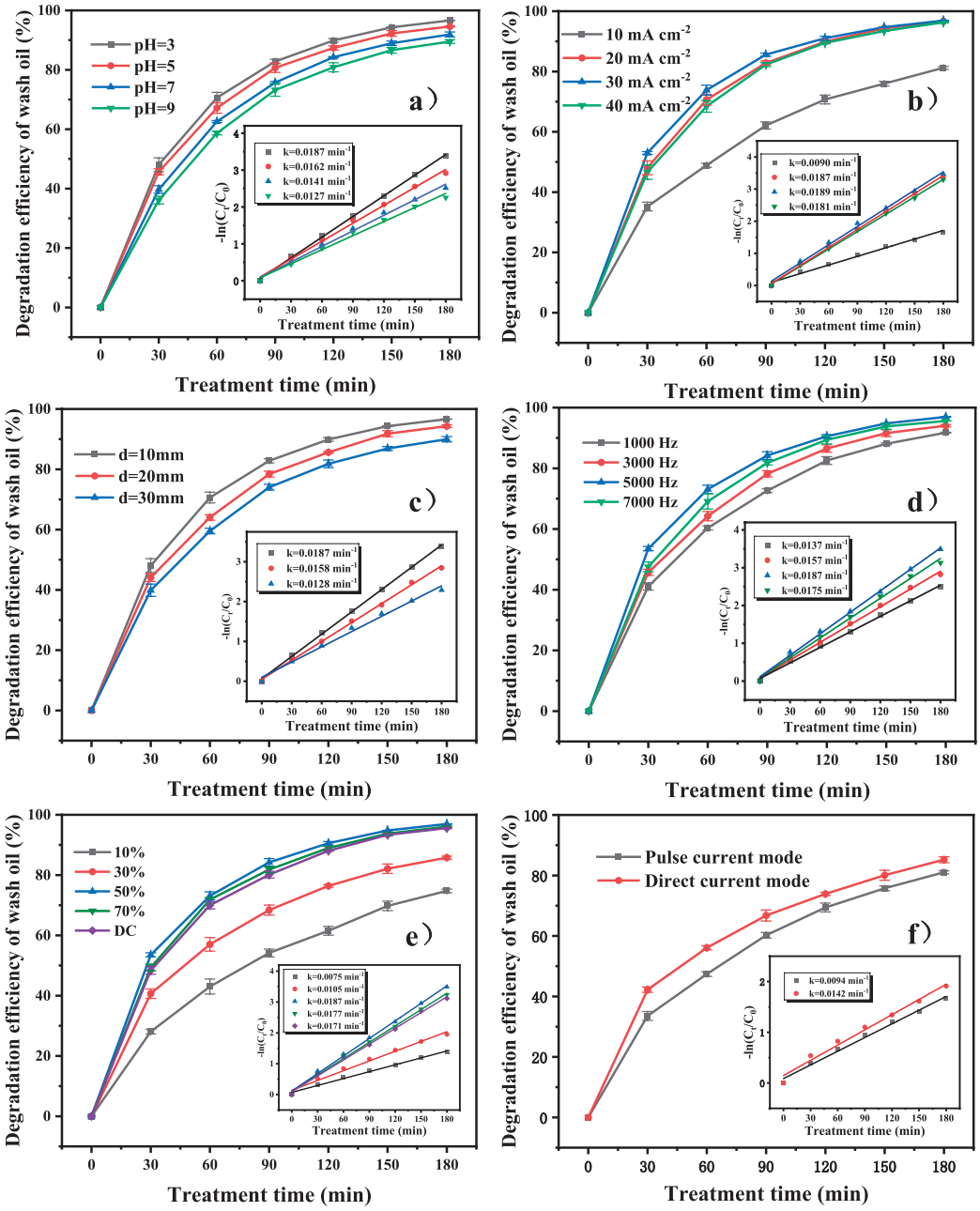

Fig. 5. Wash oil removal rates and corresponding pseudo-first-order kinetic fitting curves (illustrations) for different a) initial pH, b) current density, c) electrode spacing, d) pulse frequency, and e) pulse duty cycle. Initial conditions: current density of 20 mA cm^{-2}, electrode spacing d = 10 mm, pulse frequency of 5000 Hz, pulse duty cycle of 50%, Na_2SO_4 concentration of 0.1 mol L^{-1}; f) The removal of wash oil and the corresponding fitting curves (illustrations) under pulsed and DC power supply conditions. Among them, the current density is 10 mA cm^{-2}, and the others are the optimal conditions.

rate, which is related to the side reaction of oxygen evolution. Below the critical point, the removal rate of DC electrolytic wash oil is greater. On the contrary, the removal efficiency of the 50% pulse duty cycle is better. This may be due to the thinner diffusion layer and less oxygen precipitation in the pulse current mode, which promotes mass transfer and improves the utilization of free radicals.

In summary, the optimal conditions for pulsed electrochemical oxidation of wash oil wastewater are: pH = 3, current density is 20 mA cm^{-2}, electrode spacing is 10 mm, pulse frequency is 5000 Hz, pulse duty cycle is 50%. At this time, the highest wash oil removal was observed (95.65%).

Degradation of Different Electrodes and Different Oil Concentrations

Fig. 6a) shows the electrolysis effect of the electrode before and after modification under the above optimal conditions. By calculation, under the condition of pulse current, the degradation rate (k = 0.0187 min^{-1}) of the TiO_2-RNTs/SnO_2-Sb/PbO_2-La electrode for wash oil is 1.4 times that of the unmodified Ti/SnO_2-Sb/PbO_2 electrode. Fig. 6(b-d) show the changes of oil content, chemical oxygen demand (COD), and total organic carbon (TOC) caused by electrolysis for 180 min with initial wash oil concentrations of 100 mg L^{-1}, 50 mg L^{-1}, and 25 mg L^{-1} under the optimal pulse conditions, respectively. When the initial wash oil concentration decreased from 100 mg L^{-1} to 25 mg L^{-1}, the wash oil removal rate increased from 95.65% to 98.47%. The COD removal rate increased from 73.52% to 96.86%. The TOC removal rate increased from 64.51% to 94.62%. The treated water samples all meet the maximum allowable oil discharge concentration (5 mg L^{-1}) of wastewater specified in the pollutant discharge standard of China's petrochemical industry (GB 31571-2015). The final COD and TOC values of the water sample with an initial wash oil concentration of 25 mg L^{-1} were lower than the national emission standard (5 ppm).

It is worth mentioning that when the oil removal rate is basically stable, the removal rate of COD and TOC still increases until it tends to be stable. On the whole, an initial wash oil concentration of less than or equal to 50 mg L^{-1} with 180 min of electrolysis is appropriate for meeting the maximum allowable oil emission concentration (≤3 mg L^{-1}), COD value (≤50 mg L^{-1}), and TOC value (≤15 mg L^{-1}) in the direct discharge of the total wastewater discharge outlet of the enterprise relative to the pollutant discharge standard of China's petrochemical industry (GB 31571-2015).

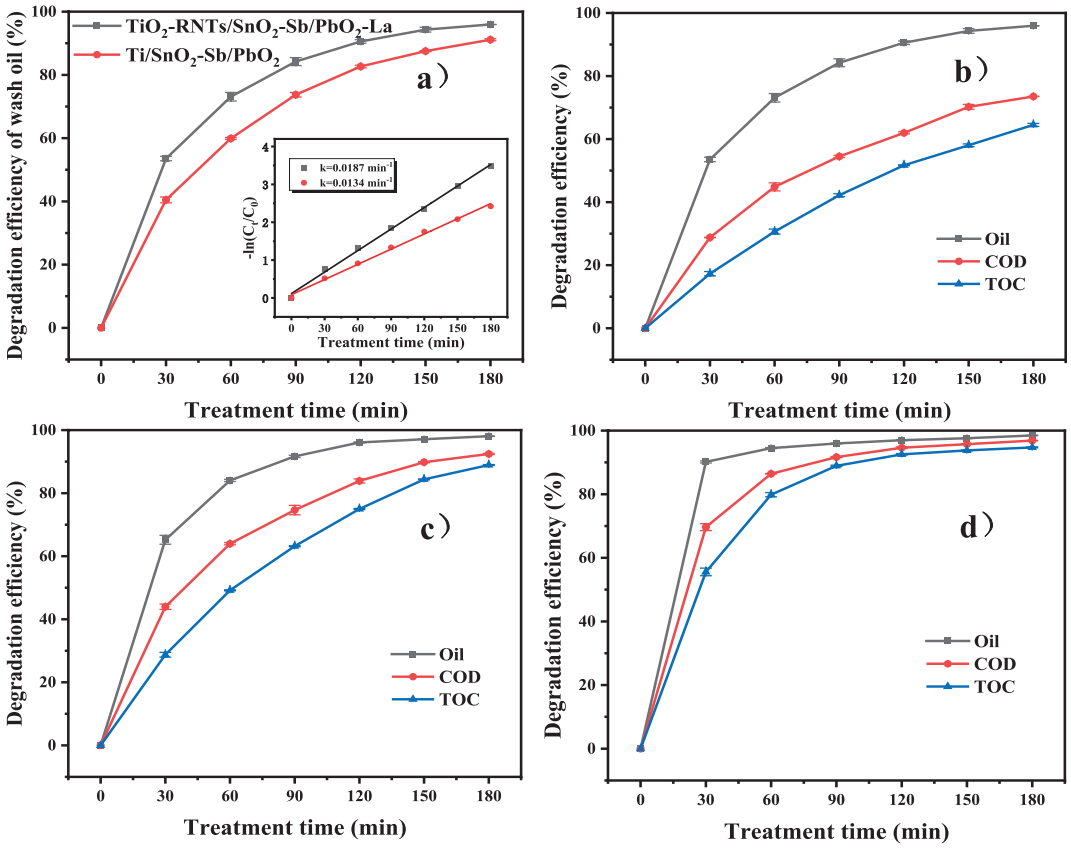

Fig. 6. a) The wash oil removal rate of the TiO_2-RNTs/SnO_2-Sb/PbO_2-La electrode and the Ti/SnO_2-Sb/PbO_2 electrode under the optimum conditions; b), c), and d) the removal rates of wash oil, COD, and TOC at different initial wash oil concentrations (100 mg L^{-1}, 50 mg L^{-1}, and 25 mg L^{-1}), respectively.

Oxidation Sequence of Organic Compounds in Wash Oil

The overlaid GC-MS chromatograms of the wash oil samples after 0, 90, and 180 min of pulsed electrochemical treatment are presented in Fig. S1. Table S1 shows that naphthalene-based polycyclic aromatic hydrocarbons (PAHs) dominated the raw wash oil, accounting for over 70% of the total peak area (2-methylnaphthalene: 30.84%; acenaphthene: 20.93%), with trace sulfur/nitrogen heterocycles as minor pollutants and no siloxanes detected. After 90 min of electrocatalytic oxidation, Table S2 shows that the original PAHs were completely degraded, with inert siloxanes (over 90% peak area, from experimental consumables/reagents) and trace small-molecule ring-opening byproducts (less than 4% peak area) as the main components, and no sulfur/nitrogen heterocycles remained. Prolonging the oxidation time to 180 min achieved deep mineralization of organic pollutants, and Table S3 shows that the small-molecule byproducts were completely oxidized, siloxanes were simplified (≈89% peak area), and only one trace oxygen-containing transition product [(Z)-4-acetyloxy-3-penten-2-one, 13.094% peak area] was identified, which could be further decomposed by hydroxyl radicals (·OH). The pollutant degradation process followed the sequence of macromolecular PAHs → small-molecule ring-opening byproducts → oxygen-containing transition products → CO_2 and H_2O.

Reproducibility and Accelerated Life Testing

The service life of the electrode is an important factor in determining whether the electrode can be used in industrial production. At low current density, the electrode has a long service life, and it is difficult to evaluate. Correa-Lozano [48] proposed an empirical relationship between actual service life and accelerated service life to evaluate the service life of electrodes at different current densities. The calculation is as follows (6):

$$T = \left(\frac{i_1}{i_2}\right)^2 T_{test} \quad (5)$$

T is the actual service life, i_1 is the current density during the test, i_2 is the current density during actual use, and T_{test} is the service life during the test. The enhanced electrode life of constant current electrolysis in 1.0 mol L^{-1} sulfuric acid solution at a high current density of 1 A cm^{-2} is shown in Fig. 7a). The TiO_2-RNTs/SnO_2-Sb/PbO_2-La electrode rapidly increases and deactivates after 960 min. The actual service life of the TiO_2-RNTs/SnO_2-Sb/PbO_2-La electrode at low current density (20 mA cm^{-2}) is 4.4 years, which is 1.3 times that of the TiO_2-RNTs/SnO_2-Sb/PbO_2 electrode and 2.4 times that of the Ti/SnO_2-Sb/PbO_2 electrode.

The stability and safety of the electrode are the basis for the environmental application of the electrochemical oxidation system. We used continuous electrolysis of wash oil to evaluate the stability of the electrode before and after modification. In Fig. 7b), after 10 cycles, the removal efficiency of the wash oil wastewater of the two PbO_2 electrodes remained basically unchanged. This proves that the PbO_2 electrode has very stable repeatability.

Since the leaching of Pb ions on the electrode surface affects the practical application of the electrode, the concentration of leached metal ions in the wastewater after electrolysis for 180 min was measured by ICP-MS and displayed in Table S4. The concentration of Pb ions precipitated from the Ti/SnO_2-Sb/PbO_2-La electrode was 89.68 μg L^{-1}. After modification, the stability of the electrode was greatly improved, the precipitation

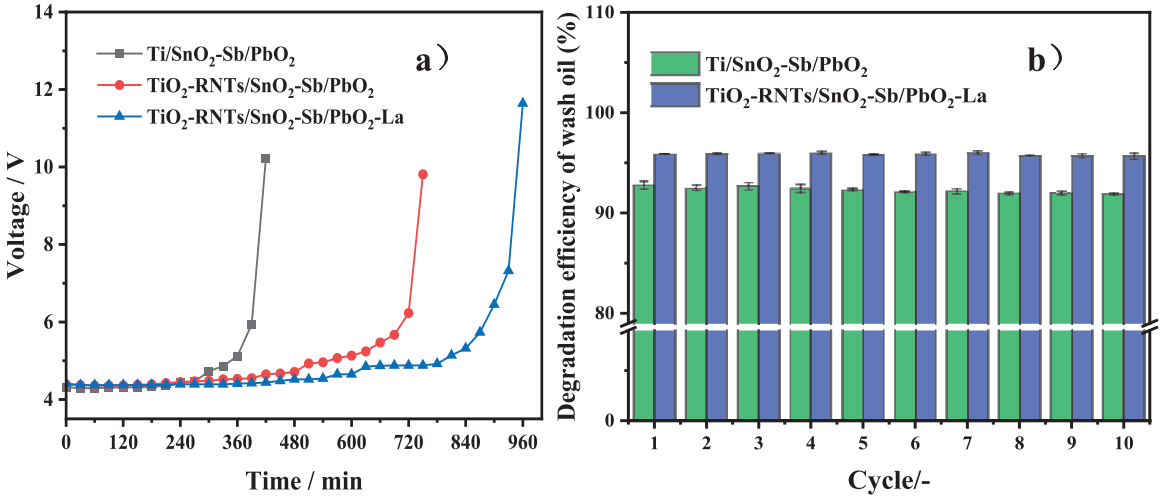

Fig. 7. a) The accelerated life test of Ti/SnO_2-Sb/PbO_2, TiO_2-RNTs/SnO_2-Sb/PbO_2, and TiO_2-RNTs/SnO_2-Sb/PbO_2-La electrodes in 1.0 mol L^{-1} sulfuric acid solution at a current density of 1 A cm^{-2}; b) Different electrodes were used for 10 cycles of electrochemical oxidation of wash oil wastewater, with each electrolysis lasting 180 min.

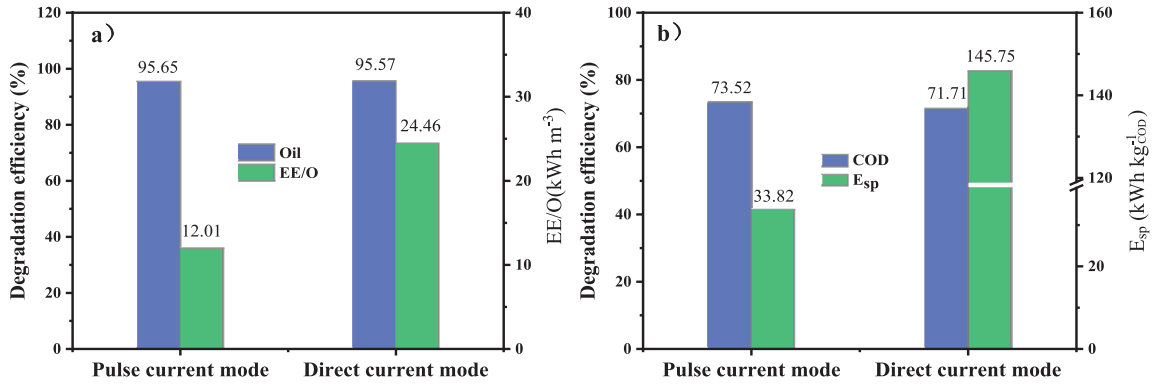

Fig. 8. a) The oil removal rate and current efficiency (EE/O); b) the COD removal rate and COD energy consumption (Esp) of 100 mg L^{-1} wash oil wastewater after 180 min of electrolysis using the TiO_2-RNTs/SnO_2-Sb/PbO_2-La electrode under different current modes.

of Pb ions was inhibited, and the concentration was 31.74 μg L^{-1}. Although the concentration of Pb ions exceeded the allowable level of public drinking water in China (≤0.01 mg L^{-1}, GB 5749-2022), it met the integrated wastewater discharge standard of China (≤0.1 mg L^{-1}, GB 8978-1996 and GB 31571-2015).

The more stable repeatability and longer service life of the modified electrode can be explained from the following aspects: (1) SEM analysis shows that the surface cracks of the modified electrode are significantly reduced, which effectively prevents electrolyte penetration and improves the service life of the electrode. (2) Electrochemical analysis shows that the introduction of TiO_2 nanotubes and the doping of La improved the OEP of the electrode, avoided the rapid deactivation of the electrode, and thus improved the service life of the electrode.

Energy Requirements

In order to evaluate the economic feasibility in practical engineering applications, under the above optimal conditions, the oil removal rate and COD removal rate after electrolysis of 100 mg L^{-1} wash oil for 180 min were taken as examples to compare the oxidation unit current efficiency (EE/O) (kWh m^{-3}) and the energy consumption per unit mass removal of COD (E_{sp}) (kWh kg^{-1}_{COD}). As shown in Fig. 8a) and 8b), the removal rates of wash oil and COD reached 95.65% and 73.52%, respectively, after 180 min of electrolysis, which is higher than that in DC mode. The EE/O value (12.01 kWh m^{-3}) in the pulse current mode is much lower than the EE/O value (26.46 kWh m^{-3}) in the DC mode, and so is the E_{sp} value. The results show that compared with direct current, pulse current electrolysis of wash oil wastewater can save 54.61% of electric energy and 76.80% of energy consumption per unit mass of COD removal. This study compares the energy efficiency of the electrochemical treatment system with other systems reported in previous literature (Table 2). The electrode pulse electrolysis method can achieve high degradation efficiency at lower energy consumption. We take the sewage treatment plant in Guizhou Province, China, which consumes an average electricity fee of CNY 0.5 per 1 kWh and can handle 10,000 tons of wastewater in one day as an example. It is calculated that the electricity cost of wastewater treatment in DC mode is CNY 122300, while the electricity cost in pulse current mode is only CNY 60050. Therefore, the TiO_2-RNTs/SnO_2-Sb/PbO_2-La electrode pulse electrochemical oxidation method is expected to improve the electrochemical treatment effect of oily wastewater while reducing unnecessary energy loss.

Table 2. Energy consumption in different electrochemical degradation systems.

Anodic materials	Target	Removal rate (%)	Time (h)	EE/O (kWh m^{-3})	E_{sp} (kWh kg^{-1}_{COD})	Refs.
TiO_2-RNTs/SnO_2-Sb/PbO_2-La	Wash oil	95.65	3.0	12.01	33.82	This work
Ti/SnO_2-Sb/PVDF-PbO_2-ZrO_2	Oily wastewater	83.33	1.67	20.09	-	[8]
Ti/SnO_2-Sb/PbO_2	Diesel fuel	85.44	2.5	33.34	-	[9]
Ti/SnO_2-Sb/Fe-PbO_2	Acid Blue 9 (AB 9)	99	2	10.93	65	[22]
PbO_2/SnO_2-Sb/TNTs-Ag/Ti	Acid Gold G (AY36)	90.57	2.5	-	96.9	[48]
Ti/SnO_2-Sb-Pt-Ru	Phenol	85	24	-	47	[51]

Conclusions

The TiO_2-RNTs/SnO_2-Sb/PbO_2-La electrode prepared by three depositions has a denser electrode surface, higher oxygen evolution potential (1.65 V), more voltammetric charge ($q^* = 70.38$ mC cm^{-2}), larger electrochemically active surface area (EASA = 138.47), lower charge transfer resistance (5.4 Ω), and longer electrode strengthening life (960 min). Under the optimum conditions, the oil removal rate was 95.65%, the COD removal rate was 73.56%, and the TOC removal rate was 64.51%. The degradation rate increased by 1.4 times, and the removal efficiency and cell voltage of the wash oil wastewater remained basically unchanged after 10 cycles. The failed electrode sheet was re-prepared into a new electrode, and the removal rate could still reach more than 95%. Compared with direct current, pulse current electrolysis of wash oil wastewater can save 54.61% of electric energy and 76.80% of energy consumption per unit mass of COD removal. Therefore, the pulse electrochemical oxidation method using the TiO_2-RNTs/SnO_2-Sb/PbO_2-La electrode is expected to improve the electrochemical treatment effect of oily wastewater and reduce unnecessary energy loss.

Acknowledgments

I would like to express my gratitude to my supervisor, Prof. Shaoqi Zhou, and Ke Zheng for their great support for my project. Thanks to their guidance and help, I was able to complete my work. I also want to thank the research team for their collaboration and help during data collection for my research project.

Conflict of Interest

The authors declare no conflict of interest.

References

1. RAYAROTH M.P., MARCHEL M., BOCZKAJ G. Advanced oxidation processes for the removal of mono and polycyclic aromatic hydrocarbons – A review. Science of the Total Environment, **857** (Pt 2), 159043, **2023**.
2. SHARMA K., VAYA D., PRASAD G., SUROLIA P.K. Photocatalytic process for oily wastewater treatment: a review. International Journal of Environmental Science and Technology, **20** (4), 4615, **2023**.
3. AYANDA O.S., ADELEYE B.O., AREMU O.H., OJOBOLA F.B., LAWAL O.S., AMODU O.S., OKETAYO O.O., KLINK M.J., NELANA S.M. Photocatalytic Degradation of Metronidazole Using Zinc Oxide Nanoparticles Supported on Acha Waste. Indonesian Journal of Chemistry, **23** (1), **2023**.
4. LV W., LI H., WANG J., WANG L., WU Z., WANG Y., SONG W., CHENG W., YAO Y. Mass Transfer-Promoted Fe^{2+}/Fe^{3+} Circulation Steered by 3D Flow-Through Co-Catalyst System Toward Sustainable Advanced Oxidation Processes. Engineering, **36**, 264, **2024**.
5. MERCHANT A.I., VAKILI A.H., KOCAMAN A., ABU AMR S.S. New advancement of advanced oxidation processes for the treatment of Petroleum wastewater. Desalination and Water Treatment, **319**, 100565, **2024**.
6. TREVIÑO-RESÉNDEZ J.D.J., MEDEL A., MEAS Y. Electrochemical technologies for treating petroleum industry wastewater. Current Opinion in Electrochemistry, **27**, 100690, **2021**.
7. LIU B., XIE C., QIAN G., ZHOU L., ZHANG C., ZHU L. Preparation of CuO-PdO-Pd/Ti electrocatalytic membrane and its performance in treating oily wastewater. Materials Science and Engineering: B, **299**, 117030, **2024**.
8. SHEN Y., LI Y., HE Y., ZHANG C., XIE C., ZHANG H., HAN E. Preparation of high performance superhydrophobic PVDF-PbO_2-ZrO_2 composite electrode and its application in the degradation of paracetamol and industrial oily wastewater. Journal of Electroanalytical Chemistry, **911**, 116231, **2022**.
9. RAJASEKHAR B., NAMBI I.M., GOVINDARAJAN S.K. Investigating the degradation of nC12 to nC23 alkanes and PAHs in petroleum- contaminated water by electrochemical advanced oxidation process using an inexpensive Ti/Sb-SnO_2/PbO_2 anode. Chemical Engineering Journal, **404**, 125268, **2021**.
10. AN Y., LEI T., JIANG W., PANG H. Research progress on photocatalytic, electrocatalytic and photoelectrocatalytic selective oxidation of 5-hydroxymethylfurfural. Green Chemistry, **26** (21), 10739, **2024**.
11. CHEN Y., TANG H., SUN H., LIU Y., XIE H., WANG L. A novel CuFe-Sb-SnO_2 anode for efficient degradation of ciprofloxacin by enhancing hydroxyl radical production: Key role of Cu/Fe in accelerating electron transfer. Separation and Purification Technology, **356**, 129996, **2025**.
12. DA COSTA P.R.F., DA SILVA D.R., MARTÍNEZ-HUITLE C.A., GARCIA-SEGURA S. Fuel station effluent treatment by electrochemical technology. Journal of Electroanalytical Chemistry, **763**, 97, **2016**.
13. DOS SANTOS E.V., SENA S.F., DA SILVA D.R., FERRO S., DE BATTISTI A., MARTINEZ-HUITLE C.A. Scale-up of electrochemical oxidation system for treatment of produced water generated by Brazilian petrochemical industry. Environmental Science and Pollution Research International, **21** (14), 8466, **2014**.
14. GARGOURI B., GARGOURI O.D., GARGOURI B., TRABELSI S.K., ABDELHEDI R., BOUAZIZ M. Application of electrochemical technology for removing petroleum hydrocarbons from produced water using lead dioxide and boron-doped diamond electrodes. Chemosphere, **117**, 309, **2014**.
15. ROSYIIDAH N.A., SETIARSO P. Nano Titanium(IV) Oxide Modified Carbon Paste Electrode for Analysis of Butylated Hydroxytoluene Concentration in Lotion by Cyclic Voltammetry. Indonesian Journal of Chemistry, **25** (4), **2025**.
16. RAHMANI A., SHABANLOO A., SHABANLOO N. A mini-review of recent progress in lead dioxide electrocatalyst for degradation of toxic organic pollutants. Materials Today Chemistry, **27**, 101311, **2023**.
17. RAI D., SINHA S. Characterization and electrochemical properties of TiO(2)-rNTs/SnO(2)-Sb/PbO(2) electrodes for the mineralization of persistent organic pollutants using anodic oxidation coupled Electro-Fenton treatment:

Effect of precursor selection. Chemosphere, **352**, 141307, **2024**.
18. ZHANG Z., LIU J., AI H., CHEN A., XU L., LABIADH L., FU M.-L., YUAN B. Construction of the multi-layer TiO2-NTs/Sb-SnO_2/PbO_2 electrode for the highly efficient and selective oxidation of ammonia in aqueous solution: Characterization, performance and mechanism. Journal of Environmental Chemical Engineering, **11** (3), 109834, **2023**.
19. CHEN M., PAN S., ZHANG C., WANG C., ZHANG W., CHEN Z., ZHAO X., ZHAO Y. Electrochemical oxidation of reverse osmosis concentrates using enhanced TiO2-NTA/SnO_2-Sb anodes with/without PbO_2 layer. Chemical Engineering Journal, **399**, 125756, **2020**.
20. NGUYEN TIEN H., MWAZIGHE F.M. Preparation of Ti/SnO(2)-Sb/La-betaPbO(2) electrode and its application in the degradation of some pollutants including prednisolone and 8-Hydroxyquinoline. Chemosphere, **333**, 138933, **2023**.
21. WANG H., XUE S., WANG W., GAO F., YI S., LI J., YANG Y., ZHAO E., WANG J., WANG J. CNTs/Ce co-doped PbO_2 anode for electro-oxidation of triclosan: Fabrication, kinetics, and degradation mechanism based on DFT calculations. Journal of Water Process Engineering, **64**, 105748, **2024**.
22. MA X., YAN Y., DAI Q., GAO J., LIU S., XIA Y. Energy-efficient pulse electrochemical oxidation of Acid Blue 9 using a Ti/SnO_2-Sb/α,β-Polytetrafluoroethylene-Fe-PbO_2 electrode: Kinetics, mass transfer and mechanism. Separation and Purification Technology, **279**, 119775, **2021**.
23. DAI Z., YU Q., CHEN Z., ZHU W., LI H., LI S., WU H., XI Q., WEI J., LI T., REN L., WANG M., LI L. Preparation and properties of MoS2 and Co double-doped modified PbO2/ZnO-NiO zinc electrowinning composite anode. Separation and Purification Technology, **354**, 128844, **2025**.
24. LIU S., GUI L., PENG R., YU P. A Novel Porous Ni, Ce-Doped PbO_2 Electrode for Efficient Treatment of Chloride Ion in Wastewater. Processes, **8** (4), 466, **2020**.
25. DOLATABADI M., EHRAMPOUSH M.H., POURNAMDARI M., EBRAHIMI A.A., FALLAHZADEH H., AHMADZADEH S. Enhanced electrocatalytic elimination of fenitrothion, trifluralin, and chlorothalonil from groundwater and industrial wastewater using modified Cu-PbO_2 electrode. Journal of Molecular Liquids, **379**, 121706, **2023**.
26. YU N., WANG Y., CAO H., SI R., XU Z., HONG X., MAO X., SHEN K., WU J. Fabrication and characterization of a novel multilayer heterojunction Si_3N_4-PbO_2 nanocomposite electrode and its application on electrocatalysis degradation of sulfathiazole. Chemical Engineering Journal, **490**, 151851, **2024**.
27. MA X., HE C., YAN Y., CHEN J., FENG H., HU J., ZHU H., XIA Y. Energy-efficient electrochemical degradation of ciprofloxacin by a Ti-foam/PbO(2)-GN composite electrode: Electrode characteristics, parameter optimization, and reaction mechanism. Chemosphere, **315**, 137739, **2023**.
28. XIA Y., DAI J., YAN Y., MA X., FENG H., DING Y. Energy-efficient electrochemical treatment of paracetamol using a PbO(2) anode based on pulse electrodeposition strategy: Kinetics, energy consumption and mechanism. Environmental Research, **216** (Pt 3), 114673, **2023**.
29. WANG X., JIANG M., YANG P., ZHOU H., XI W., DUAN J., RATOVA M., WU D., JIANG X. Recent advances in pulsed electrochemical techniques: Synthesis of electrode materials and electrocatalytic reactions. Surfaces and Interfaces, **50**, 104519, **2024**.
30. WANG J., YAO J., WANG L., XUE Q., HU Z., PAN B. Multivariate optimization of the pulse electrochemical oxidation for treating recalcitrant dye wastewater. Separation and Purification Technology, **230**, 115851, **2020**.
31. CEN Y., ZHOU Y., ZHU M., ZHENG K., ZHOU S. Preparation of the Ti/TiO(2)-RNTs/SnO(2)-Sb-Ni-La Electrode and Its Electrochemical Degradation of Oily Wastewater. Langmuir, **41** (13), 8766, **2025**.
32. CAO J., ZHAO H., CAO F., ZHANG J. The influence of F− doping on the activity of PbO2 film electrodes in oxygen evolution reaction. Electrochimica Acta, **52** (28), 7870, **2007**.
33. WU L., ZHANG C., SUN Y., WANG Y., LIAN B., CHEN Y., TU Y., WAITE T. D. Cu-mediated optimization of PbO_2 anodes for electrochemical treatment of electroless nickel plating wastewater. Chemical Engineering Journal, **450**, 138188, **2022**.
34. LI G., ZHANG L., XU P., JIANG S., BI Q., XUE J. Hydrothermal synthesis of a 3-D SnO_2 nanoflower electrode with C and N co-doped interlayer for the degradation of real cyanide wastewater. Separation and Purification Technology, **303**, 122296, **2022**.
35. DUAN T., CHEN Y., WEN Q., DUAN Y. Enhanced electrocatalytic activity of nano-TiN composited Ti/Sb–SnO_2 electrode fabricated by pulse electrodeposition for methylene blue decolorization. RSC Advances, **4** (101), 57463, **2014**.
36. IDA S., JUSTIN S.J.S., WILSON P., NEPPOLIAN B. Facile synthesis of black N-TiO_2/N-RGO nanocomposite for hydrogen generation and electrochemical applications: New insights into the structure-performance relationship. Applied Surface Science Advances, **9**, 100249, **2022**.
37. YU S., ZHANG R., DANG Y., ZHOU Y., ZHU J.-J. Electrochemical activation of peroxymonosulfate at Ti/La_2O_3-PbO_2 anode to enhance the degradation of typical antibiotic wastewater. Separation and Purification Technology, **294**, 121164, **2022**.
38. BRINK H.G., HÖRSTMANN C., PEENS J. Microbial Pb(II)-precipitation: the influence of oxygen on Pb(II)-removal from aqueous environment and the resulting precipitate identity. International Journal of Environmental Science and Technology, **17** (1), 409, **2020**.
39. LIU Y., LIU H., MA J., LI J. Investigation on electrochemical properties of cerium doped lead dioxide anode and application for elimination of nitrophenol. Electrochimica Acta, **56** (3), 1352, **2011**.
40. TRAN L.H., DROGUI P., MERCIER G., BLAIS J.F. Electrochemical degradation of polycyclic aromatic hydrocarbons in creosote solution using ruthenium oxide on titanium expanded mesh anode. Journal of Hazardous Materials, **164** (2-3), 1118, **2009**.
41. MAN S., BAO H., XU K., YANG H., SUN Q., XU L., YANG W., MO Z., LI X. Preparation and characterization of Nd-Sb co-doped SnO2 nanoflower electrode by hydrothermal method for the degradation of norfloxacin. Chemical Engineering Journal, **417**, 129266, **2021**.
42. CHEN M., WANG C., WANG Y., MENG X., CHEN Z., ZHANG W., TAN G. Kinetic, mechanism and mass transfer impact on electrochemical oxidation of MIT using Ti-enhanced nanotube arrays/SnO2-Sb anode. Electrochimica Acta, **323**, 134779, **2019**.
43. SALAZAR C., CONTRERAS N., MANSILLA H.D., YANEZ J., SALAZAR R. Electrochemical degradation of the antihypertensive losartan in aqueous medium by

electro-oxidation with boron-doped diamond electrode. Journal of Hazardous Materials, **319**, 84, **2016**.
44. LANZARINI-LOPES M., GARCIA-SEGURA S., HRISTOVSKI K., WESTERHOFF P. Electrical energy per order and current efficiency for electrochemical oxidation of p-chlorobenzoic acid with boron-doped diamond anode. Chemosphere, **188**, 304, **2017**.
45. WANG J., ZHI D., ZHOU H., HE X., ZHANG D. Evaluating tetracycline degradation pathway and intermediate toxicity during the electrochemical oxidation over a Ti/Ti(4)O(7) anode. Water Research, **137**, 324, **2018**.
46. DIAO Y., WEI F., ZHANG L., ZHAO Q., SUN H., YAO Y. The electrochemical degradation of malachite green with lead dioxide electrodes by pulse current oxidation methods. International Journal of Environmental Analytical Chemistry, **102** (5), 1126, **2020**.
47. GHAZANLOU S.I., FARHOOD A.H.S., HOSOULI S., AHMADIYEH S., RASOOLI A. Pulse frequency and duty cycle effects on the electrodeposited Ni–Co reinforced with micro and nano-sized ZnO. Journal of Materials Science: Materials in Electronics, **28** (20), 15537, **2017**.
48. CORREA-LOZANO B., COMNINELLIS C., BATTISTI A.D. Service life of Ti/SnO_2–Sb_2O_5 anodes. Journal of Applied Electrochemistry, **27** (8), 970, **1997**.
49. NGUYEN TIEN H., BUI D.N., MANH T.D., TRAM N.C.T., NGO V.D., MWAZIGHE F.M., HOANG H.Y., LE V.T. Electrochemical degradation of indigo carmine, P-nitrosodimethylaniline and clothianidin on a fabricated Ti/SnO_2–Sb/Co-βPbO_2 electrode: Roles of radicals, water matrices effects and performance. Chemosphere, **313**, 137352, **2023**.
50. LIU Y., SUN T., SU Q., TANG Y., XU X., AKRAM M., JIANG B. Highly efficient and mild electrochemical degradation of bentazon by nano-diamond doped PbO_2 anode with reduced Ti nanotube as the interlayer. Journal of Colloid and Interface Science, **575**, 254, **2020**.
51. SUN H., YAN Y., LIU Y., HOU J., CHEN Y., WANG L. Silver bridging TiO_2 nanotubes (TNTs) bases and PbO_2 active layers to accelerate electron transfer over PbO_2/SnO_2-Sb/TNTs-Ag/Ti anode for efficient organic pollutants removal. Journal of Cleaner Production, **475**, 143665, **2024**.

Appendix A. Supplementary Data

Link to Appendix A. https://www.pjoes.com/SuppFile/220125/1/